

Asynchronous accelerator with RFQ injection for active longitudinal compression of accelerated bunches

A.R. Tumanyan^(*), Yu.L. Martirosyan^(*), V.C. Nikhogosyan^(*), N.Z. Akopov^(*),
Z.G. Guiragossian^(**), R.M Martirosov^(*), Z.N. Akopov^(*)

(*) Yerevan Physics Institute (YerPhI), Yerevan, Br. Alikanian St.2, 375036, Republic of Armenia
(**) Guest Scientist at YerPhI

Abstract

An asynchronous accelerator is described, in which the principle of its operation permits the active longitudinal bunch compression of accelerated proton beams, to overcome the space charge limitation effects of intense bunches. It is shown that accelerated bunches from an RFQ linac can be adapted for Asynchronac injection for a multiple of choices in the acceleration frequencies of the RFQ and the Asynchronac. The offered new type of accelerator system is especially suitable to accelerate proton beams for up to $100MeV$ energy and hundreds of mA average current.

1 Introduction

According to its principle of operation, the asynchronous accelerator (Asynchronac) can be viewed to be a machine in between the following two cases. The Asynchronac can be viewed as a linear accelerator wrapped into a spiral, in which the harmonic number of the acceleration voltage and the equilibrium phase of a bunch relative to the acceleration field can be changed independently. Also, it can be viewed as a separate orbit cyclotron (SOC) [1][2][3] and an asynchronous cyclotron, which has been described earlier [4][5].

It is simpler to present the concept of the Asynchronac as a modification of the parameters and the operating mode of a separate orbit cyclotron, without changing its structure (see *Figure1*). If R , the radius and f , the acceleration voltage frequency in a SOC are selected to be large, such that q , the harmonic number between acceleration cavities is a large integer at injection:

$$q = \frac{h}{N_c} = \frac{2\pi R f_{rf}}{N_c V} \quad (1)$$

(where, N_c is the number of resonators in a cyclotron stage and V is the speed of particles), q would decrease during acceleration as the speed of particles increased, presenting the following possibilities.

First, it is possible to restrict the increase of radii from injection to ejection orbits, by not limiting the increase of the average radius of the machine. Second, it becomes possible to reduce the strength of the bending magnetic fields without restrictions. Third, it is possible to increase the length of drift spaces between bending magnets. And fourth, it becomes possible to independently set the RF equilibrium phase during the acceleration process.

Thus, the creation of non-isochronous or asynchronous mode of SOC operation is provided by having the inter-cavity harmonic number, q discretely change on integer values as the beam transits through the sectors and turns. By modifying the magnetic path length in the sectors the hopping of integer q values is accomplished. These are the modifications of the parameters and the operating mode of a separate orbit cyclotron, which convert it to become an Asynchronac, with additional new useful qualities. One such important quality is now the ability to axially compress and thus to monochromatize the accelerated proton or ion beam bunches.

Only at low energies rapid changes occur in the speed of particles. Because it is now possible to hop over integer values of q in a reasonably sized accelerator radius, the Asynchronac concept can best be applied at energies below 100 *MeV*, to produce average beam currents in the hundreds of *mA*. Such accelerators, in addition to their stand-alone use for specific applications, can be more useful as the initial injector stage for the production of intense bunches, which are injected into higher energy proton accelerators, such as synchrotrons, linacs or cyclotrons, to produce high and super-high energy intense beams.

In the present study a valuable implementation of the Asynchronac concept is based on the multiple use of modern RFQ linacs (generating large currents at small energy spread) [6].

2 Conditions to creat bunch compression in the asynchronac

The creation of bunch compression in an Asynchronac is made possible by the inherently available independent setting of the RF acceleration equilibrium phase, from one resonator to another. In this case, the continuous differential equation for synchrotron oscillations does not apply. Consequently, the value of the equilibrium phase in each resonator is determined by the expression:

$$\cos \varphi_e = \frac{2\Delta E_s \pm \Delta E_r}{2U_n T_z \sin \Psi} \quad (2)$$

In equation (2) φ_e is the acceleration phase for the synchronous particle in a bunch and ΔE_s is the half width of the natural energy spread of particles, induced in a bunch, ΔE_r is the full width of the desired energy spread to be induced in a bunch as it passes through the periodic resonators.

In an injected bunch, a particle having a higher energy than the energy of the synchronous particle is found normally at the head of the bunch and those having lower energy than the central one are normally at the tail. For this normal case, ΔE_r is used with the plus sign in equation (2). However, for the reverse situation where particles having higher energy than the synchronous particle appear at the tail of the bunch, ΔE_r in equation (2) is used with the minus sign.

U_n is the amplitude of the acceleration voltage in the n-th resonator. Using electrical and mechanical methods to regulate each cavity channel, the details of which will be described in a separate paper, the acceleration field in any n-th sector resonator's particle orbit channel can be independently tuned. In equation (2) 2Ψ is the full phase width of a bunch and T_z is the transit-time factor determined by

$$T = \frac{\sin \Delta\Phi/2}{\Delta\Phi/2} \quad (3)$$

where,

$$\Delta\Phi = \frac{2\pi f_{rf} L_{gap}}{\beta c} \quad (4)$$

f_{rf} is the frequency of the acceleration field in resonators, L_{gap} is the full acceleration gap in resonators, β is the relativistic velocity factor, c is the speed of light. Normally T_z can be maintained at a constant value if the acceleration gap in a resonator is increased in proportion to the speed of the accelerated beam, which in turn reduces the need to increase the amplitude of the acceleration voltage U_n .

The energy gain of a central particle in the bunch ΔE_e after exiting a resonator, is given by

$$\Delta E_e = U_n T_z \sin \varphi_e \quad (5)$$

The energy gain for an edge particle, a , located at the head of the bunch and an edge particle, b , located at the tail of the bunch are determined by

$$\Delta E_a = U_n T_z \sin(\varphi - \Psi) \quad (6)$$

$$\Delta E_b = U_n T_z \sin(\varphi + \Psi) \quad (7)$$

The equilibrium phase for acceleration is set within the limits of

$$0 < \varphi_e < \left(\frac{\pi}{2} - \Psi\right) \quad (8)$$

so that the phase of off-center particles always remains below $\pi/2$, and a Gaussian bunch distribution is maintained.

The bunch duration τ_f at the end of any sector (at the space located between two adjacent resonators) is given by

$$\tau_f = \tau_s + \Delta\tau \quad (9)$$

$$\Delta\tau = \frac{S_s}{c} \left(\frac{1}{\beta_b} - \frac{1}{\beta_a} \right) \quad (10)$$

where $\tau = \Psi T/\pi$, S_s is the orbital path length of particles in the sector and T is the RF period duration.

In equation (10) if a positive sign is obtained for $\Delta\tau$, which is when $\beta_a > \beta_b$, this describes bunch elongation and an increase in τ_f , and if a negative sign is obtained, it describes axial bunch compression, with a corresponding decrease in the value of τ_f .

The last case is possible only for the reverse particle configuration, which is when $\beta_a < \beta_b$. Here the normal positioning of particles in a bunch is altered. The particles a , at the head of a bunch, now have smaller energy with respect to particles at the center and the tail, a second condition that supports bunch compression to occur.

If in equation (9) a negative sign is obtained for τ_f , it means that over-compression has occurred, after which the normal distribution of particles in a bunch will be restored.

If in a bunch, conditions are found by the proper selection of the equilibrium phase to constantly support the reverse particle distribution, the bunch duration will constantly decrease and overcome the space charge effect, which drives the elongation and transverse expansion of the bunch.

From equation (10) it is evident that to obtain large and negative values of $\Delta\tau$ it is necessary to have large sector path lengths, S_s and a large negative difference in the reciprocals of β . These are the third and fourth conditions to achieve bunch compression in the Asynchronac.

The values of beam injection energy E_i , initial energy spread $\Delta E_{s,i}$, injected beam emittance, bunch duration $\tau_{s,i}$, the injection radius R_i , the number of acceleration cavities N_c , the amplitude of acceleration voltage U_n and the RF frequency f_{rf} , are selected during the conceptual design of the accelerator, based on various technical feasibility considerations. These parameters must φ_e selected beforehand, based on the simultaneous solution of equations (9), (10), (5) and (2), to determine the required value of the acceleration equilibrium phase φ_e , so that it produces bunch compression in a given sector and a specific orbital turn.

However, the analytical solutions of the combined equations appear sufficiently cumbersome. Consequently, these cannot be reproduced here, but are found in the computer codes for the calculation and optimization of these parameters.

The control algorithm for the steering of bunches from one sector to the other in the Asynchronac is as follows. As a function of the measured energy spread $\Delta E_{s,i}$ of the injected beam, the duration of bunches τ_i , the design value of the mean path length of the beam in the first sector S_{s1} and the selected RF acceleration voltage in the first resonator, the RF phase is set, such that an equilibrium phase φ_e is produced on the rising side of the acceleration voltage, which after the passage of a bunch in the first resonator will cause at once the inversion of particles to occur.

Also, this particle inversion must be sufficiently intense, to reduce the duration of bunches τ_{f1} close to zero at the end of the beam orbit in the first sector. Thus, there are two cases, one which conserves the inverted distribution, and the other which induces over-compression and then restores the normal distribution of particles in a bunch.

For the first case, to obtain a monoenergetic beam in the follow-on second sector, it is necessary to adjust the path length of particles in the first sector S_{s1} and to set the equilibrium phase in the second resonator, so that the acceleration takes place on the falling side of the RF field. For the second case, the rising side of the RF voltage is used to obtain a beam of zero energy spread. In this case ΔE_s in equation (2) takes on a negative sign and ΔE_r is set to zero. In the desired case of preserving inverse distribution of particles, it is necessary to work only on the rising side of the RF acceleration field. The choices are determined by the magnitude of ΔE_s .

Hence, at the start of the second sector the beam will be monoenergetic and have a bunch length equal to τ_{f1} , and at the end of the sector the bunch duration τ_{f2} will increase due to the space charge effect. At the same time this provides the possibility to estimate the effect experimentally.

The equilibrium phase at the third resonator must be set such that the acceleration occurs again on the rising side of the RF voltage, to obtain an inverse particle distribution in bunches, so that at the end of the third sector the bunch duration τ_{f3} reduces again to almost zero. Thus, the process repeats itself, with and without alternating the acceleration mode on the rising and falling side of the RF voltage. For a more graphic presentation the numerical modeling in the following section is provided.

The path length of particles in sectors is set by the parameters of the bending magnetic system, which essentially must change from sector to sector, to provide the desired values of q and φ_e . To have the possibility of

precise tuning and to relieve the maintenance of different mechanical tolerances of the accelerator components and their alignment, we propose to place in the sectors different correction elements. This is in addition to the magnetic lenses for transverse focusing of the beam and a number of beam monitors. In particular, wiggler type magnets will be installed in the straight sections to correct the path length of particles. Finally, evaluations show that in having large beam orbit separation steps and in the other features of the Asynchronac, the mechanical tolerances of accelerator elements and their alignment are relatively relaxed, in the order of 10^{-3} .

The important relaxation of tolerances in the Asynchronac is one of its main advantages, in comparison to other similar accelerator structures, namely, as compared with the isochronous separate orbit cyclotrons [1][2]. In these the necessity of strictly maintaining the isochronism of particle motion reduces to having tight tolerances, which in practice are difficult to implement. Other important advantages are due to the features of longitudinal bunch compression and strong transverse focusing. As such, it is possible to consider the acceleration of bunches at an equilibrium phase close to 90^0 , which in turn, increases the efficiency of acceleration, decreases the number of turns, decreases the beam losses, and increases the number of accelerated particles in bunches.

Basically, the Asynchronac's deficiency is the uniqueness or unprecedented nature of the sector bending magnetic system. This complicates the standardization of their manufacture and tuning, and somewhat increases the initial commissioning time and manufacturing cost of the accelerator. However, some technical innovations already made, essentially facilitate the solution of these problems. This concern, the fabrication of magnet yokes from iron sheets with the ability to mechanically change the magnetic lengths and the remote control of the magnetic alignment in each sector and turn. The individual feeding of the DC bending magnets and partially the magnetic focusing lenses is straightforward to implement, using modern electronics and computers.

The issues of beam transverse focusing in this study are not considered, since known standard solutions can be utilized, as normally found in strong focusing synchrotrons. In particular, the separate function periodic magnetic structure can be of the FODO type. In the Asynchronac the main difference will be the possibility of having a slowly changing betatron oscillation fre-

quency, in going from one period to another. This will allow to compensate the frequency shift of these oscillations, which is due to different effects, including the space charge effect.

3 Configuring RFQ beams for injection into cyclotron

The method of forming short duration bunches from modern high frequency RFQ's, which produce large current and small energy spread beams, can be modified to produce longer duration bunches at longer inter-bunch spacing, that becomes acceptable for injection in the lower frequency Asynchronac. This technique is based on time compressing the RFQ-produced beam, in which the compression is completed downstream, at the point of injection into the Asynchronac, as described in *Figure2(a)*. *Figure2(b)* shows the resulting single longer bunch produced from a train of shorter RFQ-produced bunches.

Our proposed scheme to produce the required beam compression is as follows. RFQ-produced bunches are initially steering in a RF deflector with a saw-tooth time varying voltage. The saw-tooth period is equal to the period of the Asynchronac's driving RF frequency. The sequentially more and more deflected bunches pass through a 180° shaping magnet with different path lengths, as seen in *Figure2(a)*. After which all RFQ bunches within the saw-tooth period coincide at the time focal point, producing full compression of the bunch train into a single longer bunch, at the injection point of the Asynchronac. The RF deflector and the injection point of the Asynchronac are located at conjugate points about the 180° shaping magnet.

If the duration of the short bunches in a RFQ is designated by τ_{RFQ} and the period between RFQ bunches is T_{RFQ} , the time-compression of the bunch train produces a single longer bunch τ_{cyc} for injection into the Asynchronac, given by

$$\tau_{cyc} = m\tau_{RFQ} \tag{11}$$

where the period between injected bunches will be

$$T_{cyc} = mT_{RFQ} \tag{12}$$

in which m is the number of RFQ bunches in a train length equal to the period of the driving saw-tooth ramped voltage.

The path length of any k -th bunch in the train, starting from the RF deflector up the time-focused injection point of all the idealized paths, is obtained by

$$L_k = 2\left[\frac{a}{\cos \alpha_k} + R(1 - \cos \alpha_k + \frac{\pi}{2} - \alpha_k) - \text{atg}\alpha_k + b\right] \quad (13)$$

under the conditions of

$$R \geq (\text{atg}\alpha_{\max}) \text{ and } b \leq (R \cos \alpha_{\max}) \quad (14)$$

The significance of the quantities R , a , b , α are exhibited in the geometry of *Figure2(a)*.

The maximum path length of particles will be

$$L_{\max} = 2\left[a + b + \left(\frac{\pi R}{2}\right)\right] \quad (15)$$

while the minimum path length is

$$L_{\min} = 2\left[\frac{a}{\cos \alpha_{\max}} + R\left(\frac{\pi}{2} - \alpha_{\max}\right)\right] \quad (16)$$

The separation of maximum and minimum path lengths, under the optimum condition of

$$R = \text{atg}\alpha_{\max} \text{ and } b = R \cos \alpha_{\max} \quad (17)$$

will be

$$\Delta L_{\max} = 2R[\text{ctg}\alpha_{\max} + \cos \alpha_{\max} + \alpha_{\max} - \text{cosec} \alpha_{\max}] \quad (18)$$

However, from primary considerations, the separation of maximum and minimum path lengths is

$$\Delta L_{\max} = \beta c T_{\text{cyc}} \quad (19)$$

Knowing the value of ΔL_{\max} from equation (19) and inverting equation (18) produces the optimal turning radius R_{tr} of beam tracks in the time compression shaping magnet, whereby the overall dimensions and the magnetic field strength are obtained. Thus, the optimum bending radius is given by

$$R_{tr} = \frac{0.5\Delta L_{\max}}{ctg\alpha_{\max} - \cos e c\alpha_{\max} + \cos \alpha_{\max} + \alpha_{\max}} \quad (20)$$

4 Results of numerical calculations

A numerical example is worked out to present the key performance features and to indicate a rough cost estimate of the Asynchronac. The following parameters are used in the calculation of the numerical example accelerator model. The RFQ linac's RF system operates at 350 MHz , producing a proton beam of 2.0 MeV energy, an energy spread of $\Delta E_s = 2\%$ and a CW current of up to 100 mA . The frequency of the acceleration voltage in the Asynchronac is chosen to be 50 MHz , i.e. to have a seven-fold difference in the frequencies of the acceleration fields, between the RFQ and the Asynchronac. This means that the number of RFQ bunches to be compressed into a single bunch is $m = 7$.

However, in our example calculation, in order to be able to use two funneled RFQ's for injection, we have assumed 14 bunches to be compressed into a single bunch for injection, and for the maximum steering angle of the RF deflector, $\alpha_{\max} = 20^\circ$ is selected.

Whereby, the following parameter values are obtained

$$\begin{aligned} \tau_{cyc} &= 4.0 \text{ ns} \quad T_{cyc} = 40.0 \text{ ns} \quad \Delta L_{max} = 78.2 \text{ cm} \\ R &\approx 35.15 \text{ cm} \quad b \approx 33.0 \text{ cm} \quad a = 96.6 \text{ cm} \end{aligned}$$

The total maximal path length including the magnetic shaping structure will be 330 cm , and the track length up to the middle of the first resonator will be approximately 4.4 m . The duration of bunches at the end of the total path length will increase due to the beam's energy spread ΔE_s , by approximately 2.2 ns , so that the bunch length in the first resonator of the Asynchronac will be

$$\tau_{cyc} = 4.0 + 2.2 = 6.2 \text{ ns}$$

In the given example of the Asynchronac, operating at a RF acceleration frequency of 50 MHz , the inter-bunch separation is $T_{cyc} = 20 \text{ ns}$. To match with this spacing, the use of two RFQ's will be required, each injecting at an inter-bunch spacing of 40 ns , which when initially combined in a RFQ funnel [7], will yield the required 20 ns inter-bunch spacing.

Incidentally, the Asynchronac geometry permits further increasing the number of injector RFQ linacs in a manner analogous to the conventional method of multi-turn injection. RFQ's with own bunch-train compressors can inject beams at each sector of the first or subsequent turn. However, each must have a different injected beam energy that matches the orbit's energy at the point of injection. Thus, successive RFQ's must have correspondingly higher beam energies.

The bunch-train-compressed beam from a RFQ injector, through the 180° bending magnet enters the Asynchronac's first resonator. *Figure 1* schematically depicts the Asynchronac structure and the beam orbits, only for the central particles of the first three turns. The orbit radius at injection is $R_i = 3.0m$, the orbit-to-orbit separation is $\Delta R = 25cm$ and the number of resonators is $N_c = 4$. The number of sectors is also equal to $N_s = 4$ per beam turn, and since the number of turns is 17, the number of independent channels and magnets is $4 \cdot 17 = 68$.

The key design parameters of the Asynchronac for the numerical example are summarized in *Table 1*. Room temperature resonators are used in the design, which increase the machine's radius. Following the development and operation of modern cyclotron resonators at the Paul Scherrer Institute [8] and the related designs and models [9], the operation of these resonators at RF frequencies of $40 - 50 MHz$ and peak voltages of up to $1.1 MV$ can be made available. These resonators have a length of approximately $6 m$, height of $3 m$ and width along the beam of $0.3 m$, and provide a radial operating clearance for orbits of up to $4 m$.

Table 1. Key Parameter Values of an Asynchronac

	PARAMETER	UNIT	VALUE
	Beam Spacie		Proton
E_i	Injected Beam Energy	MeV	2.0
E_e	Extracted Beam Energy	MeV	50.0
R_i	Injected Beam Radius	m	3.0
R_e	Extracted Beam Radius	m	7.0
N_c	Number of Acceleration Cavities		4
N_m	Number of Sector Magnets		66
H	Field Strength in Sector Magnets	T	0.11 – 0.85
ΔE	Energy Gain per Turn	MeV	0.04 – 3.60
ΔR	Orbit Turn-to-Turn Separation	cm	25.0
n	Number of Turns		16.5
h	Harmonic Number		52 – 58
L_m	Length of Sector Magnets	m	0.75 – 5.13
L_f	Length of Drift Spaces	m	2.2 – 9.7
τ_f	Duration of Bunches	ns	6.2 – 0.5
N_0	Number of Protons per Bunch		$2.5 \cdot 10^{10}$

Thus, an injected bunch duration of 6.2 ns is compressed down to 2.5 ns at the end of the first sector, using the parameter values of $U_n = 130 \text{ KeV}$, $T_z = 0.95$, $\varphi = 55.8^\circ$ and setting the equilibrium phase in the first resonator at $\varphi_e = 18.4^\circ$. Under these conditions, particles at the head of the bunch will have energy equal to 2.104 KeV , while at the tail of the bunch, particle energy will be 1.975 KeV . Particles at the equilibrium phase will have an energy of 2.039 KeV and the energy spread of the bunch will be $\Delta E_s = 2.104 \text{ KeV}$. Next, particle inversion will take place. At the end of the first sector, $\Delta\tau$ will be 8.9 ns , consequently $\tau_f = 6.2 - 8.9 = -2.7 \text{ ns}$, whereby the inversion has been completed and over-compression has occurred. The subsequent processes are easier to observe in *Figures 3 – 10*, right up to the achievement of the final proton beam energy of approximately 50 MeV , which is produced after 16.5 turns in the Asynchronac.

It is observed from the numerical results in these figures, that the process of effective longitudinal beam compression has terminated after the first three turns. The duration of bunches has attained an almost stationary value of about 0.5 ns and the final energy spread of the beam ΔE_s ends up to be zero in the Asynchronac.

We now roughly estimate the maximum particle population in a proton

bunch, as a function of bunch shortening. In our simplified approach we ignore the intra-beam scattering and wake field effects on bunch lengthening and the axial focusing from the RF acceleration cavities. In the proton bunch's rest frame, the energy spread due to the bunch electric self-field is given by

$$\frac{\Delta P^2}{2m} = -e \int E_z dz \quad (21)$$

where z is the longitudinal coordinate and ΔP is the momentum spread. The longitudinal space-charge electric field of the bunch is obtained as [10]

$$E_z = -\frac{e}{4\pi\epsilon_0} \frac{1}{\gamma^2} \left(1 + 2 \ln \frac{b}{a}\right) \frac{\partial \lambda(z)}{\partial z} \quad (22)$$

where ϵ_0 is the absolute dielectric constant, a and b are the radii of the proton beam and the vacuum chamber, respectively, and $\lambda(z)$ is the particle linear density in the bunch. Taking a Gaussian distribution for the bunch linear density

$$\lambda(z) = \frac{N_0}{\sqrt{2\pi}\sigma} e^{-\frac{z^2}{2\sigma^2}} \quad (23)$$

with $\sigma = 0.7z$ as the standard value of the bunch length, and inserting expression (22) into equation (21), and after integration within the bounds of the bunch's initial z_i and final z_f half-lengths, the following formula is obtained for the maximum particle population in a bunch

$$N_0 = \frac{\Delta P^2}{2m} \frac{4\pi\epsilon_0}{e^2} \frac{\gamma^2}{e^{-\frac{z_f^2}{2\sigma^2}} - e^{-\frac{z_i^2}{2\sigma^2}}} \frac{\sqrt{2\pi}\sigma}{1 + 2 \ln \frac{b}{a}} \quad (24)$$

Using the parameters in the above, and taking for the beam radius $a = 0.5$ cm and the vacuum chamber radius $b = 5.0$ cm, the estimated maximum number of protons per bunch is $N_0 \approx 5 \cdot 10^{11}$.

From these figures it is seen that the magnetic field in each sector and turn has sufficiently different and not necessarily optimized parameters. To simplify the numerical calculations we assumed that the bending magnets in each sector and turn consist of single whole units, instead of being a number of shorter modular magnets that would serve the required purpose. In making the conceptual design of a specific Asynchronac, the sector and

turn magnets will be modularized with optimized parameters, such that the differences among modular magnets will be few, to permit standardizing the manufacturing process.

Rather low values of $0.1 - 0.85$ *Tesla* are required for the magnetic field strength in each sector and turn. The fabrication of small-sized modular bending magnets at these field strengths is a standard matter. Should the beam's vacuum chamber need an aperture full width of as much as 10 *cm*, this can be easily accommodated, since the turn-to-turn orbit separations will all be equal at $\Delta R = 25$ *cm*. The lengths of the remaining free drift spaces in sectors and turns, after the allocation of resonators and bending magnets, will be more than 2.0 *m*. This will allow not only to freely install focusing magnetic elements and beam monitoring apparatus, but also to provide easily 100% extraction of the beam.

A rough estimation of the cost to build and operate the Asynchronac shows that the cost per megawatt of proton beam produced from the Asynchronac is much less expensive by an order of magnitude, as compared to a megawatt of proton beam produced from the high and super-high energy accelerators.

5 Conclusion

The primary objective of this paper is to show that the innovated accelerator type, which we refer to as the Asynchronac, has sufficient feasibility features for its implementation, in which an accelerated proton beam of up to 100 *MeV* energy and hundreds of *mA* current can be effectively bunch-compressed. Consequently, it is important to expedite the extension of further multifaceted studies on this concept, to improve the quality of future machines for scientific and applied applications, potentially using this alternative.

References

- [1] J. A. Martin et. al. *The 4-MeV Separated-Orbit Cyclotron*, IEEE Transactions on Nuclear Science, v. NS-16, N3, part 1, p.479, 1969

- [2] U. Trinks, *Exotic Cyclotrons - Future Cyclotrons*, CERN Accelerator School, May 1994, CERN Report 96-02, 1996
- [3] O. Brovko et.al. *Conceptual Design of a Superferric Separated Orbit Cyclotron of 240 MeV Energy*, Proceedings of the 1999 Particle Accelerator Conference, vol. 4, p. 2262, Brookhaven, NY
- [4] A. R. Tumanian, Kh. A. Simonian and V. Ts. Nikoghosian, *Powerful Asynchronous Multi-Purpose Cyclotron*, Physics Proceedings of the Armenian National Academy of Sciences, No. 4, vol. 32, p. 201, 1997, Yerevan, Armenia
- [5] A. R. Tumanyan, G. A. Karamysheva and S. B. Vorozhtsov, *Asynchronous Cyclotrons*, Communication of the Joint Institute for Nuclear Research, Report E9-97-381, 1997, Dubna, Russia
- [6] A. Schempp, H. Vorrman. *Design of a High Current H- RFQ Injector*, Proceedings of the 1997 Particle Accelerator Conference, vol. 1, p. 1084, Vancouver, B.C., Canada; A. Lombardi et al. *Comparison Study of RFQ Structures for the Lead Ion Linac at CERN*, Proceedings of EPAC, Berlin, 1992
- [7] K.F.Johnson et. al. *A Beam Funnel Demonstration; Experiment and Simulation*, Particle Accelerator Conference, Vols.37-38, p.261, 1992
- [8] *Proceedings of the LANL Workshop on Critical Beam Intensity Issues in Cyclotrons*, Santa Fe, NM, December 4-6, 1995, p.358
- [9] N. Fietier and P. Mandrillon, *A Three-Stage Cyclotron for Driving the Energy Amplifier*, Report CERN/AT/95-03(ET), Geneva, 1995
- [10] H.Wiedeman, Particle Accelerator Physics, v.2, p.344, 1995

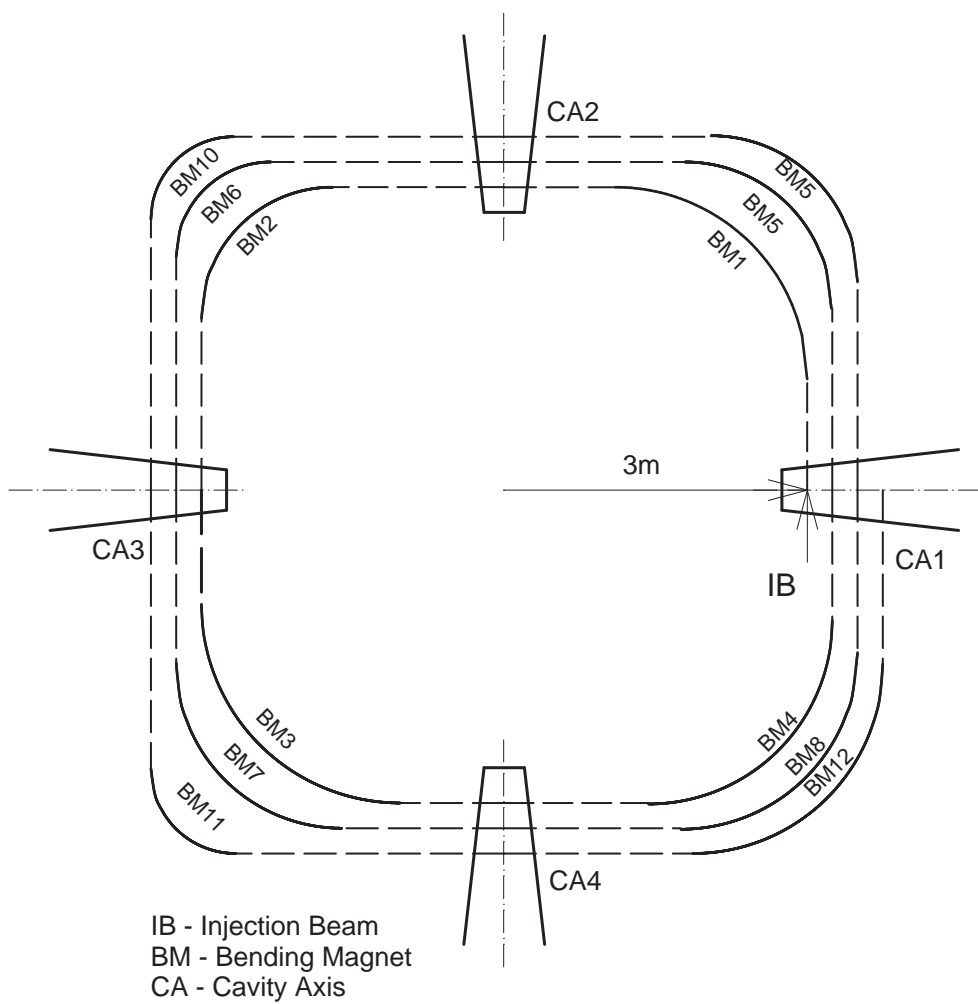


Figure 1 Trajectory of central particle in Asynchronac on first three turn

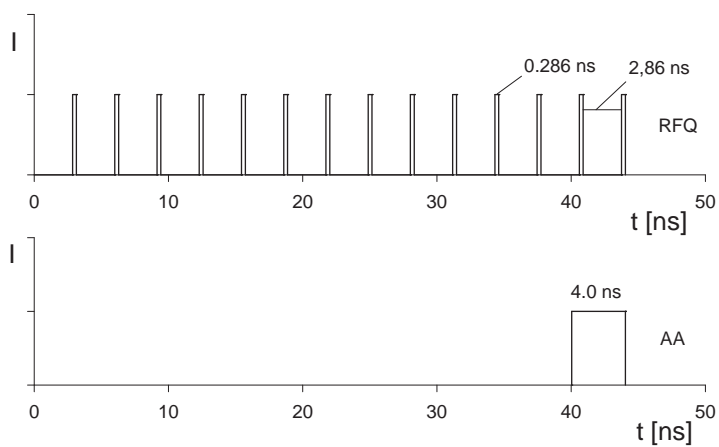
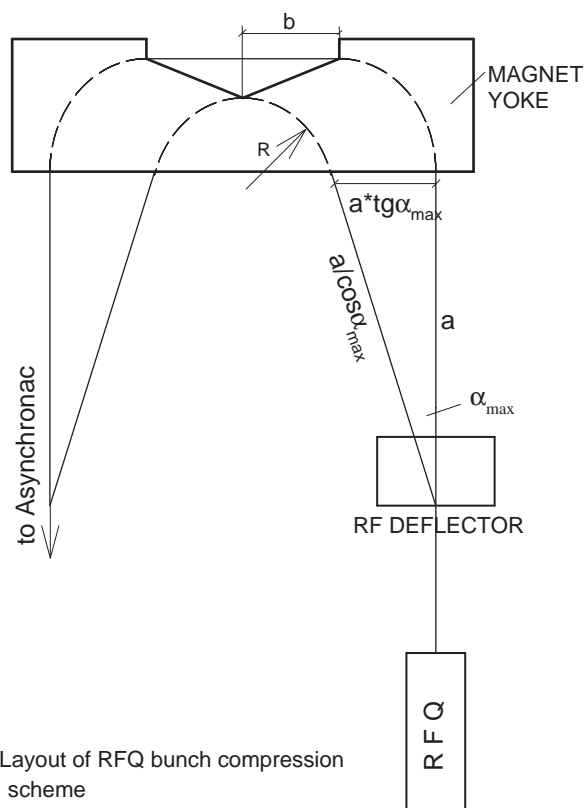


Figure 2a Layout of RFQ bunch compression scheme

Figure 2b RFQ and Asynchronac bunch time sequence

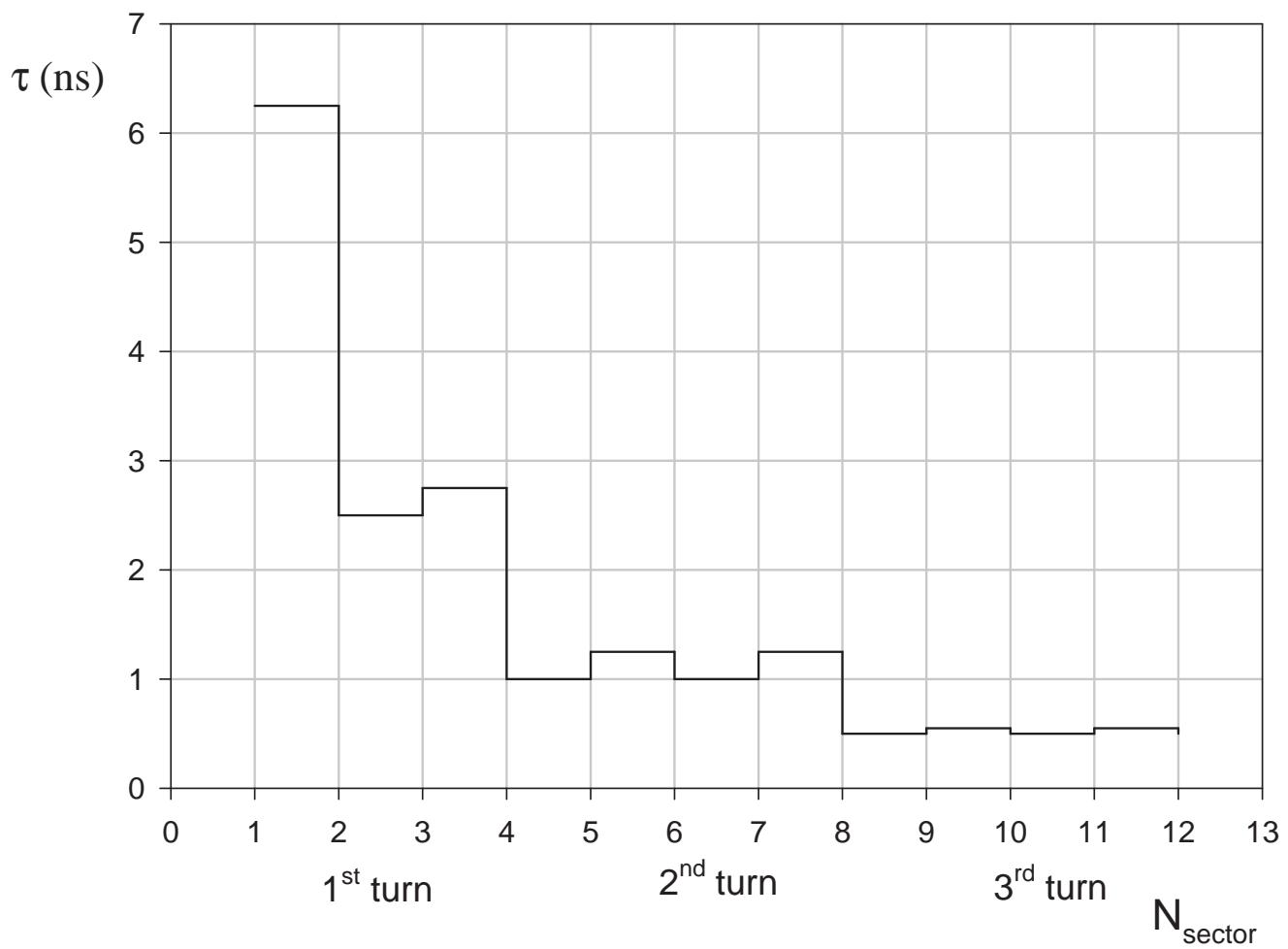


Figure 3 Bunch duration

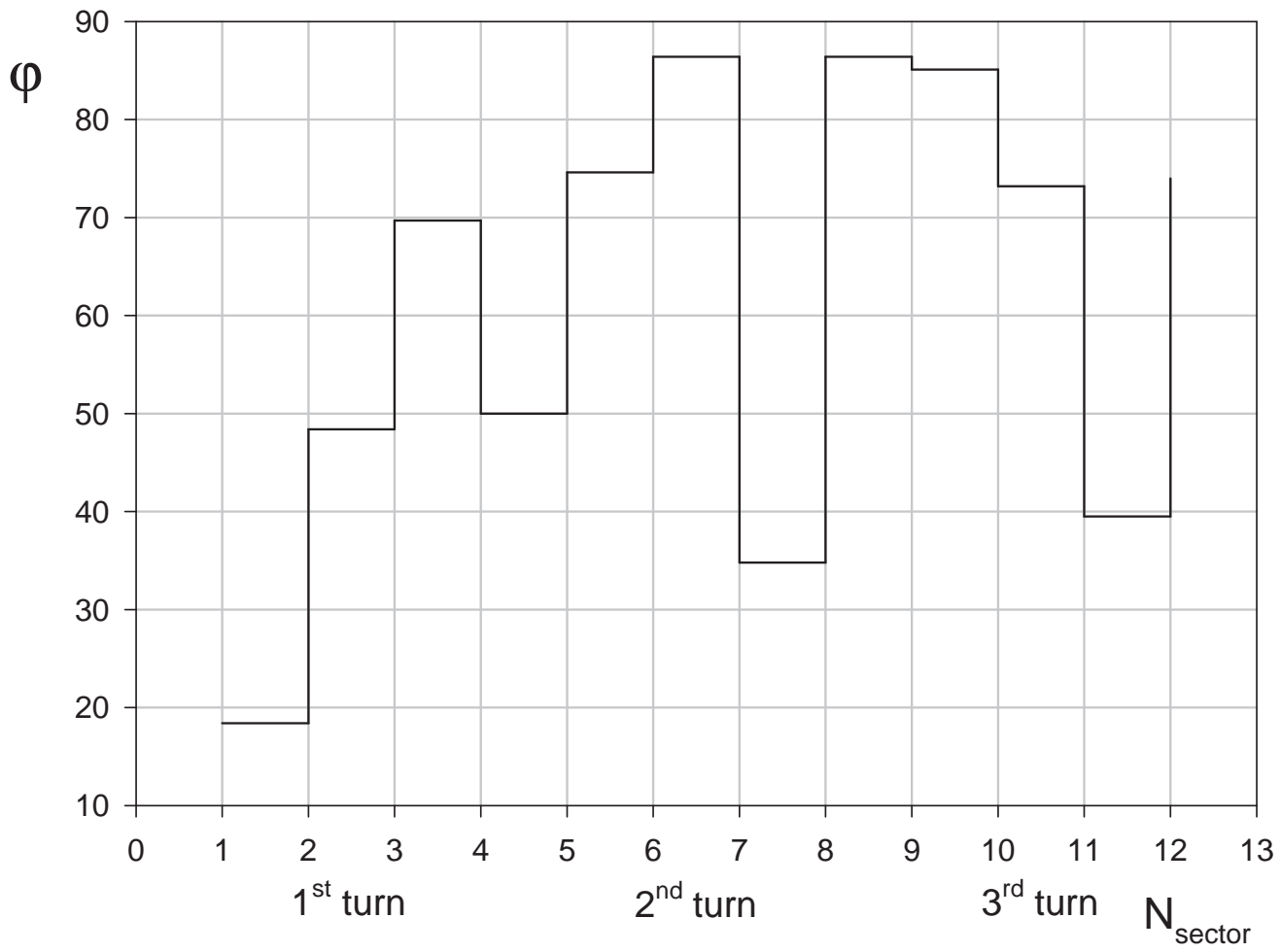


Figure 4 Acceleration equilibrium phase

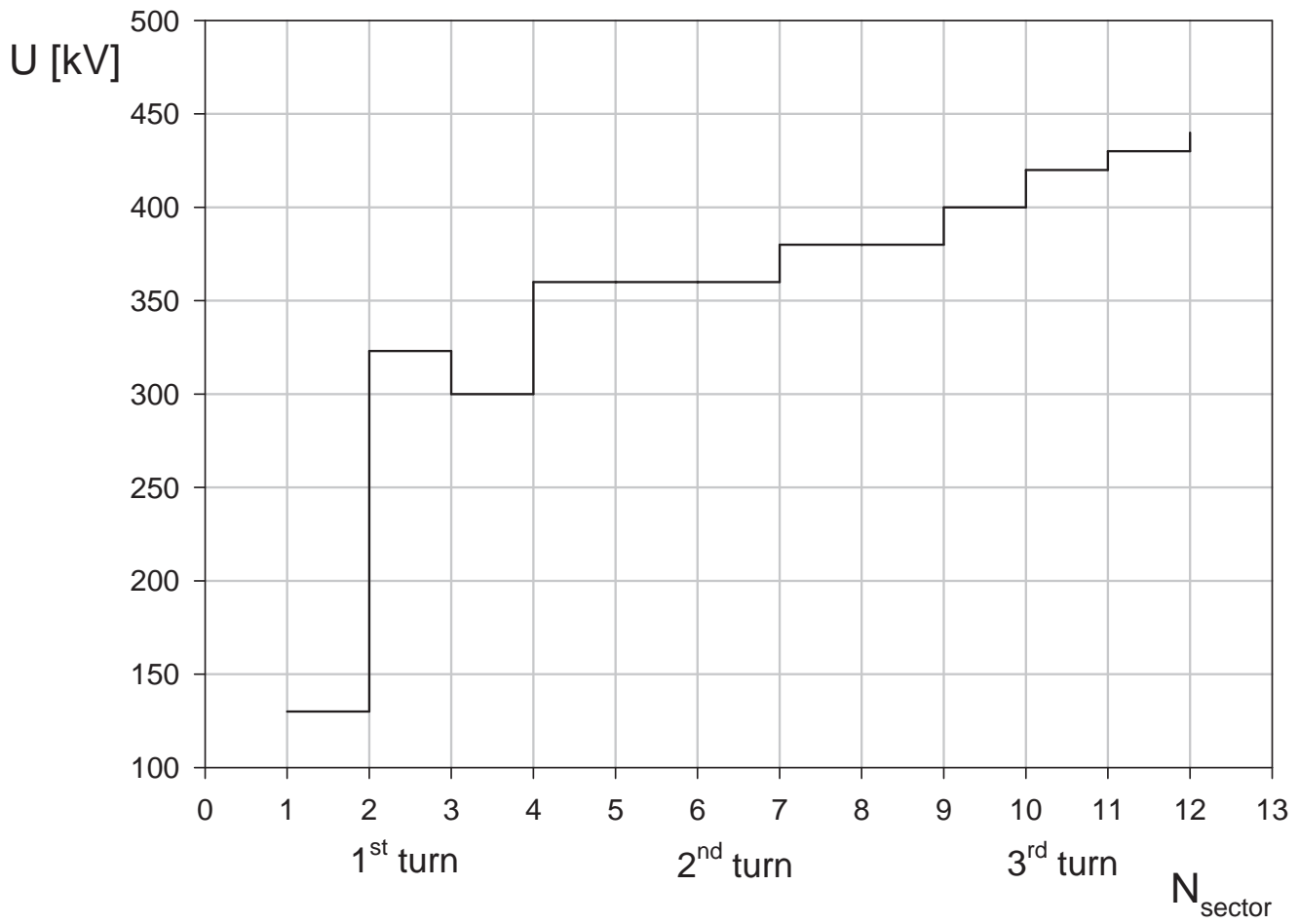


Figure 5 Acceleration voltage amplitude

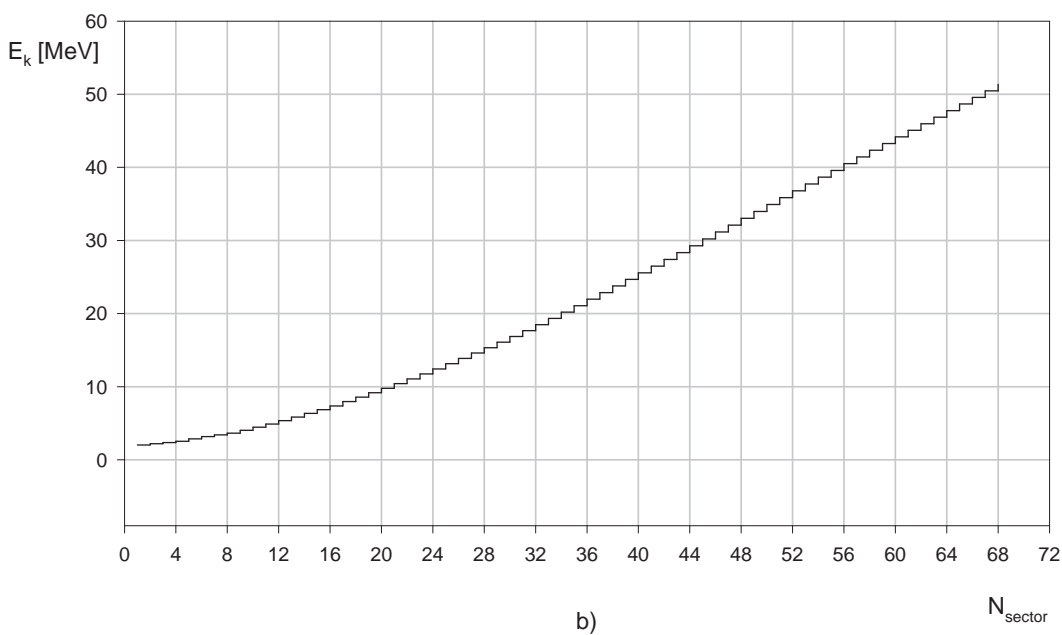
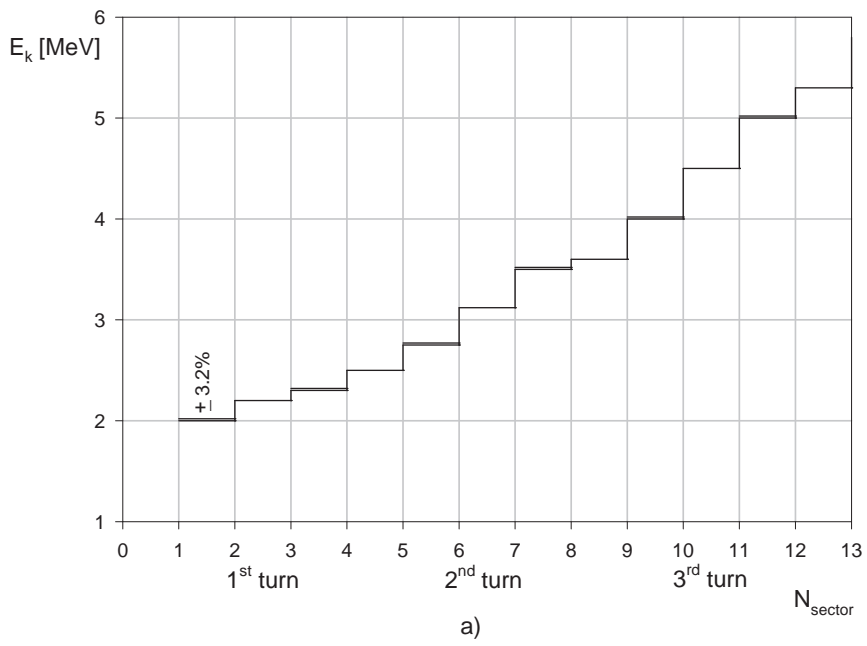


Figure 6 (a,b) Kinetic energy

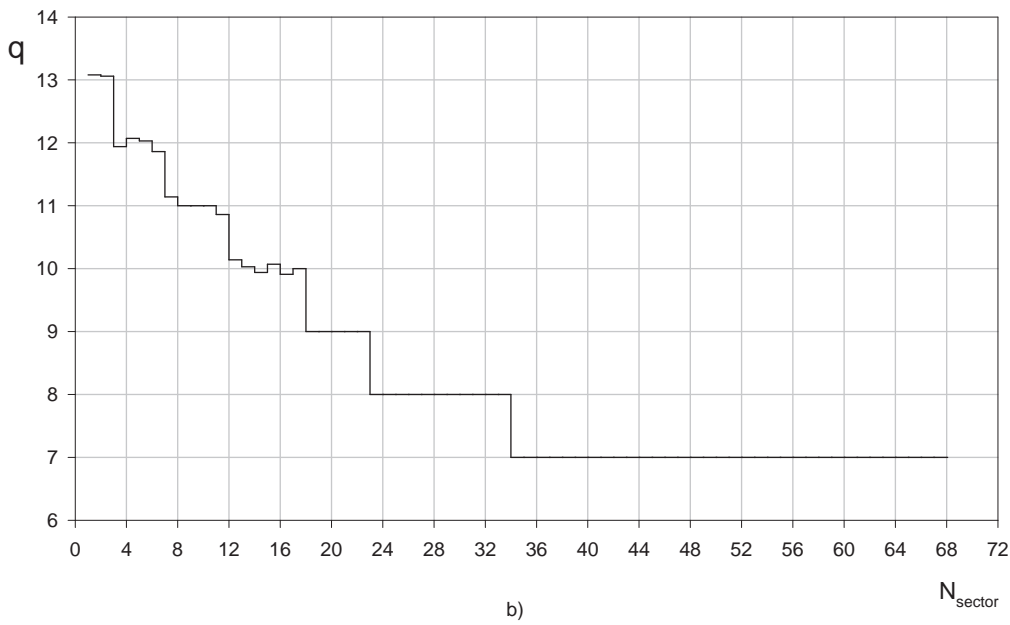
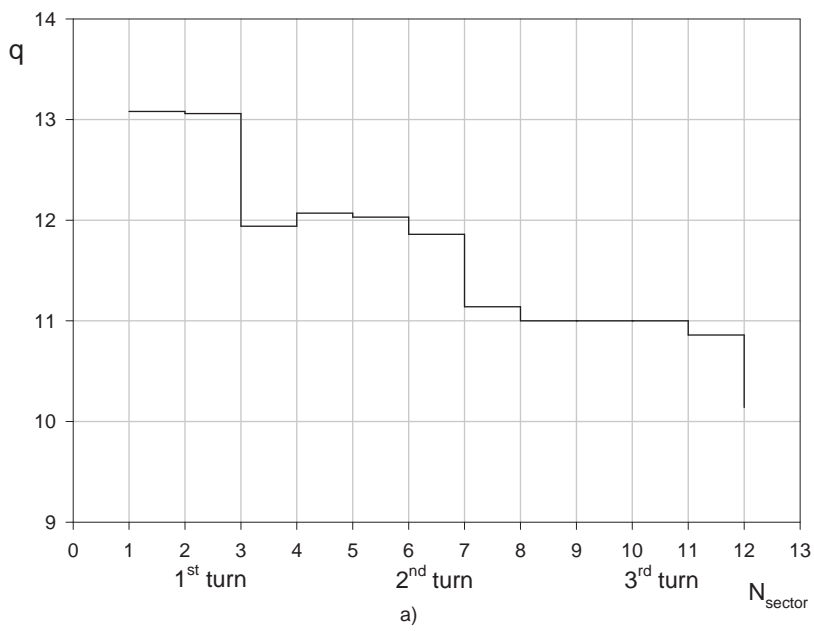


Figure 7 (a,b) Intercavity harmonic number

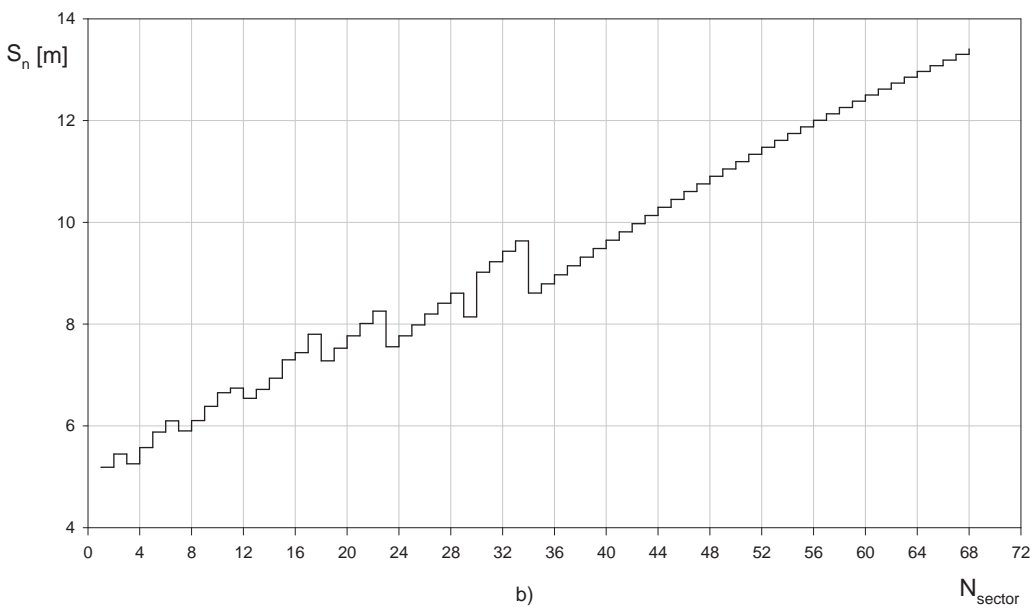
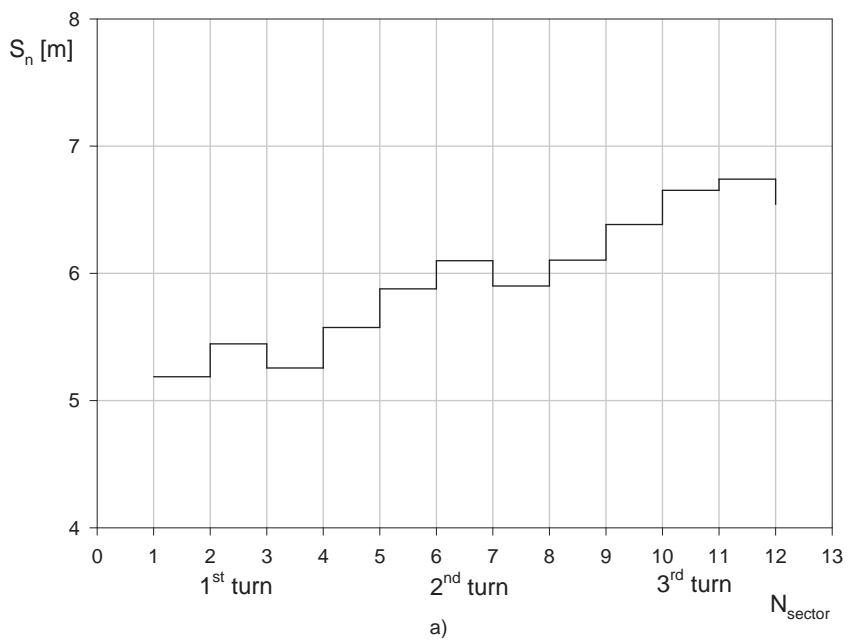


Figure 8 (a,b) Beam trajectory length

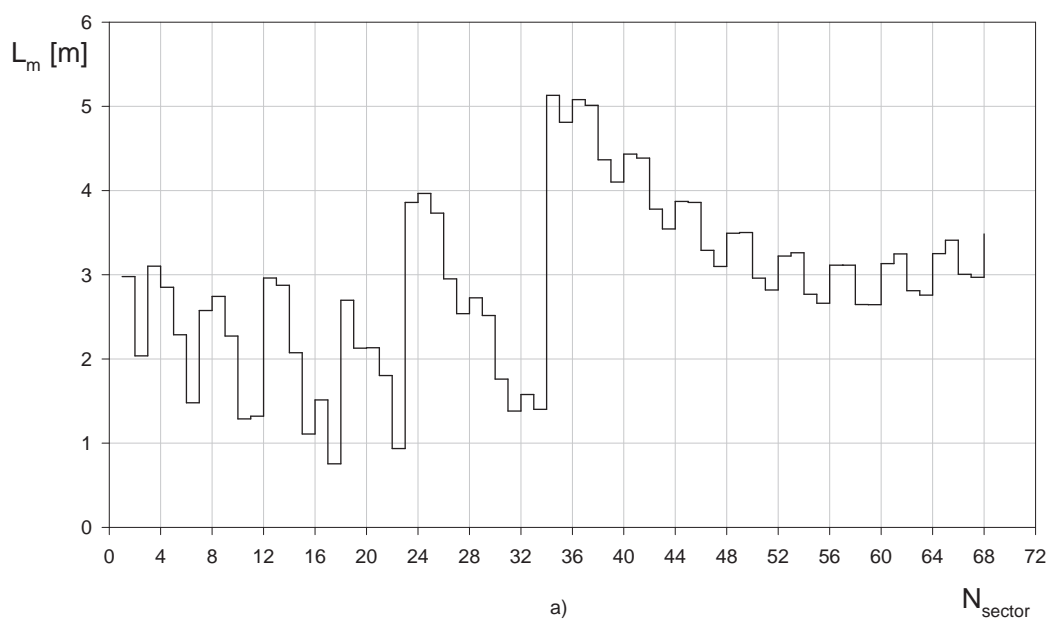
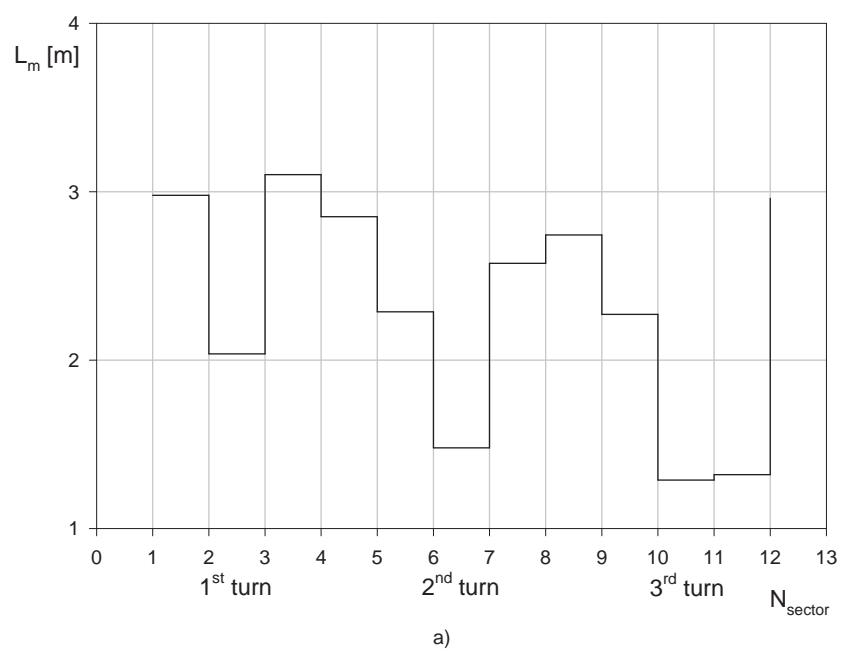


Figure 9 (a,b) Length of sector magnets

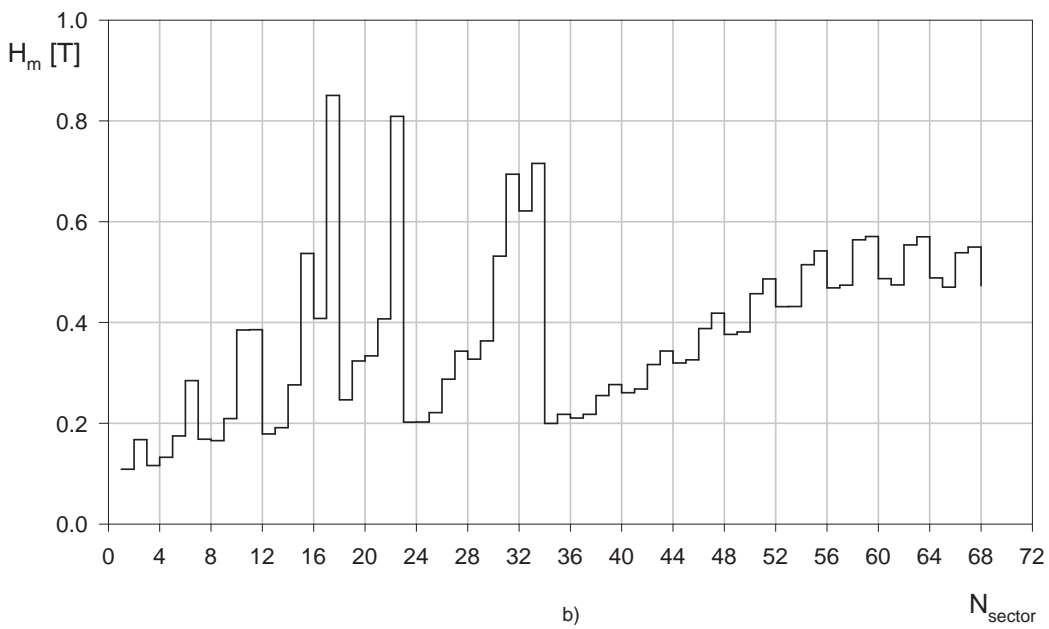
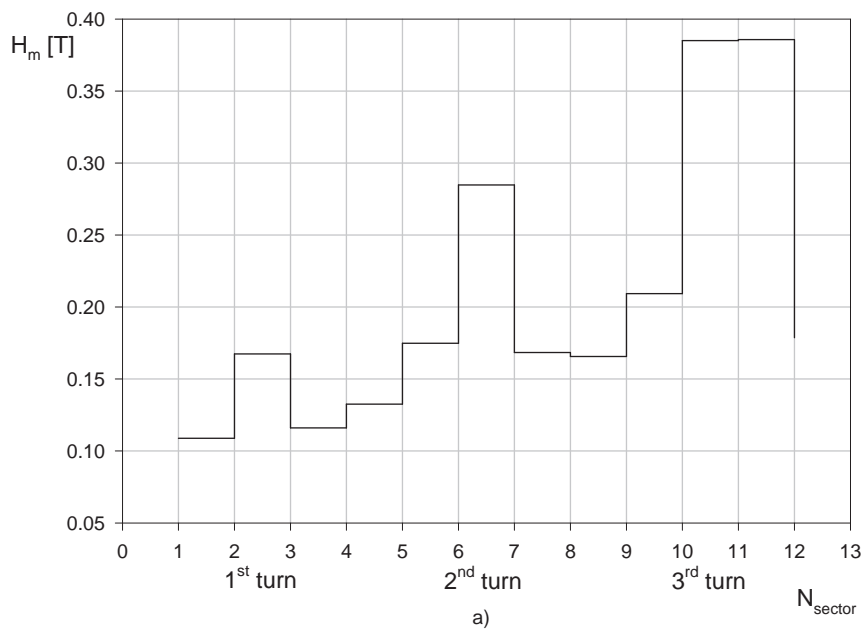


Figure 10 (a,b) H-field in sector magnets